Arch. Metall. Mater. **64** (2019), 1, 421-430

DOI: 10.24425/amm.2019.126268

J. WIDŁASZEWSKI*#, M. NOWAK*, Z. NOWAK*, P. KURP**

LASER-ASSISTED THERMOMECHANICAL BENDING OF TUBE PROFILES

The subject of the work is the analysis of thermomechanical bending process of a thin-walled tube made of X5CrNi18-10 stainless steel. The deformation is produced at elevated temperature generated with a laser beam in a specially designed experimental setup. The tube bending process consists of local heating of the tube by a moving laser beam and simultaneous kinematic enforcement of deformation with an actuator and a rotating bending arm. During experimental investigations, the resultant force of the actuator and temperature at the laser spot are recorded. In addition to experimental tests, the bending process of the tube was modelled using the finite element method in the ABAQUS program. For this purpose, the tube deformation process was divided into two sequentially coupled numerical simulations. The first one was the heat transfer analysis for a laser beam moving longitudinally over the tube surface. The second simulation described the process of mechanical bending with the time-varying temperature field obtained in the first simulation. The force and temperature recorded during experiments were used to verify the proposed numerical model. The final stress state and the deformation of the tube after the bending process were analyzed using the numerical solution. The results indicate that the proposed bending method can be successfully used in forming of the thin-walled profiles, in particular, when large bending angles and a small spring-back effect are of interest.

Keywords: laser forming, laser-assisted bending, numerical modelling

1. Introduction

Over many decades, bending of tubular parts has been widely researched due to their mass application in automotive, aerospace, shipbuilding and energy industries. Several tube-bending phenomena and problems, such as thinning or cracking of the tube wall, neutral layer shifting, spring-back and ovalization of the tube cross-section have been deeply studied in order to estimate optimal technological parameters [1,2]. It is well known that inappropriate process parameters can lead to unwanted wrinkling phenomenon, especially for large diameter and thin-walled tubes [3].

Investigations aimed at flexible, precise and cost-effective forming methods must take into account challenges present in manufacturing of thin-walled components, which are made of high-strength and difficult-to-form materials, sometimes in small batches. To avoid or reduce the involved problems several innovative tube bending techniques are under development. One of them is non-contact laser bending of tubes. Forming is performed by scanning the material surface with a moving laser beam, without any application of external forces [4,5]. Plastic deformation is produced due to the thermal expansion of the material under conditions of restraint deformation and due to the action of the resulting internal forces at elevated temperature [6,7]. Hence, the hard and difficult-to-form materials can be equally easily bent as other materials. The method is flexible, because it does not require product-specific dies, mandrels and similar traditional hard tooling [8]. Forming can be performed on a multi-purpose laser stand, controlled by a software with product-specific input parameters. The method has been investigated for manufacturing critical aircraft components made of Inconel 718 nickel-based superalloy [9,10]. Unfotunately, the non-contact bending process is time-consuming, being an incremental forming technology, in which the final change of shape is accumulated from numerous small deformations.

The current study is an attempt to combine effects of localised laser heating with the action of external forces to achieve efficient tube bending with the reduction of unwanted effects. Incorporating laser heating into bending of thin-walled components renders new prospects for manufacturing not only the prismatical profiles, but also the conical and other components, for which the use of inductive heating is difficult. Presented investigation was a part of a project aimed at development of a novel flexible forming process for the small-batch products in the aerospace industry.

One of the traditional bending techniques is the Rotary Draw Bending (RDB), in which the deformation is obtained by forcing the clamped profile to accommodate the shape of

* INSTITUTE OF FUNDAMENTAL TECHNOLOGICAL RESEARCH, POLISH ACADEMY OF SCIENCES, 5B PAWIŃSKIEGO STR., 02-106 WARSAW, POLAND
** KIELCE UNIVERSITY OF TECHNOLOGY, DEPARTMENT OF INDUSTRIAL LASER SYSTEMS, 7 TYSIĄCLECIA PAŃSTWA POLSKIEGO AV., 25-314 KIELCE, POLAND
# Corresponding author: jwidl@ippt.pan.pl

a rotating die [11]. However, this technique is constantly struggling with problems such as large spring-back or wrinkling. In the paper [12] the authors proposed the new RDB process, in which the tube is pre-heated before bending. Another technique that uses thermal softening of the material is bending with the local induction heating [13,14].

As far as the authors have determined, no previous investigation has been made on the laser-assisted bending of tubes. With the exception of laser-assisted hydroforming [15], very few works have concerned the combined action of laser heating and mechanical load in forming of tubes to date. Hsieh and Lin [16] studied the buckling mechanism in laser forming of tubes with axial preload. Jamil et al. [17] analysed small bending deformation (bend angle up to about 2 deg) of elastically pre-stressed and laser-heated micro-tubes made of pure nickel. The tubes were mechanically pre-deformed in a cantilever arrangement to increase the laser bending effect with compressive pre-stress in the irradiated region. A short pulse heating (up to 20 ms) by a stationary laser beam was applied.

The method presented in this work is an improvement of the technique described in [18] and [19]. The new method uses a non-oscillating laser beam with rectangular cross-section, instead of the oscillating one with circular cross-section. The formerly applied guiding rollers with vertical axes have been replaced by the rollers with horizontal axes. In addition, a new laser power control system was used to stabilize material temperature at the laser spot, significantly reducing the influence of local changes in material absorptivity.

2. Materials and methods

A dedicated experimental set-up was built to investigate bending of thin-walled profiles with the application to laser heating. Experimental investigations were conducted using the X5CrNi18-10 stainless steel tube of the nominal diameter 20 mm and wall thickness 1 mm. The measured initial wall thickness of the samples was in the range from 0.89 to 1.02 mm, with the mean value of 0.94 mm.

Deformation of the tube sample was enforced by guiding rollers, a bending arm and an actuator, which was attached to the end of the tube (Fig. 1). The laser head (6) was placed in the plane of bending (4), so that the heat was delivered to the region of high bending stress and desired deformation.

In order to control material temperature during the process, a pyrometer was used, which measured the surface temperature at the centre of the laser spot (Fig. 2). The rectangular laser spot (20 mm × 2 mm) covered the whole width of the tube. The temperature measurement system was integrated with the laser

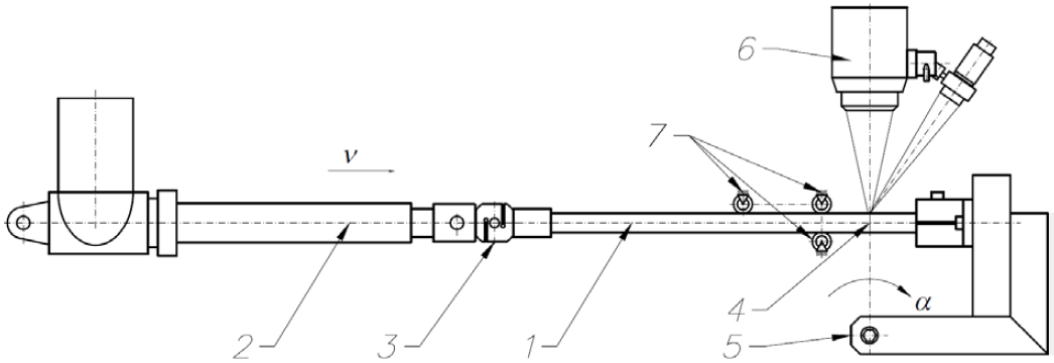

Fig. 1. A scheme of the experimental setup for the laser-assisted tube bending process. 1 – tube, 2 – actuator, 3 – force sensor, 4 – plane of bending, 5 – bending arm, 6 – laser head, 7 - roller with horizontal axis

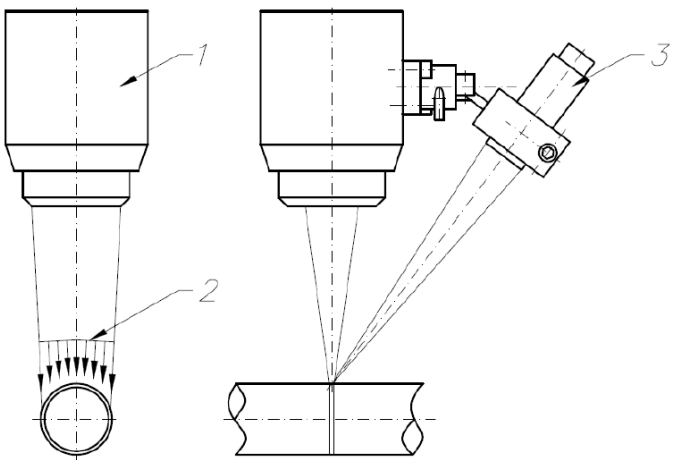

Fig. 2. A scheme of laser heating and temperature measurement system: 1 – laser head, 2 – laser beam, 3 – pyrometer

source, which allowed laser power control with the feedback loop, so that the constant material temperature at the laser spot was maintained by updating the laser power in real time.

The tube sample was placed on the test stand, as shown in Fig. 3. One end of the tube was connected to a computer-controlled electro-mechanical actuator and the other one was clamped in the bending arm (Fig. 3a). During the experiment, the actuator pushed the end of the tube over the distance $u = 160$ mm (Fig. 4). The free end of the tube followed the motion of the bending arm, which enforced the bending deformation. The final configuration of the tube is shown in Fig. 3b.

After the deformation process had finished, and the tube has cooled down, it was removed from the testing stand and two perpendicular dimensions of it in the selected cross-sections were measured. The employed description of configuration of the sample is shown in Fig. 4.

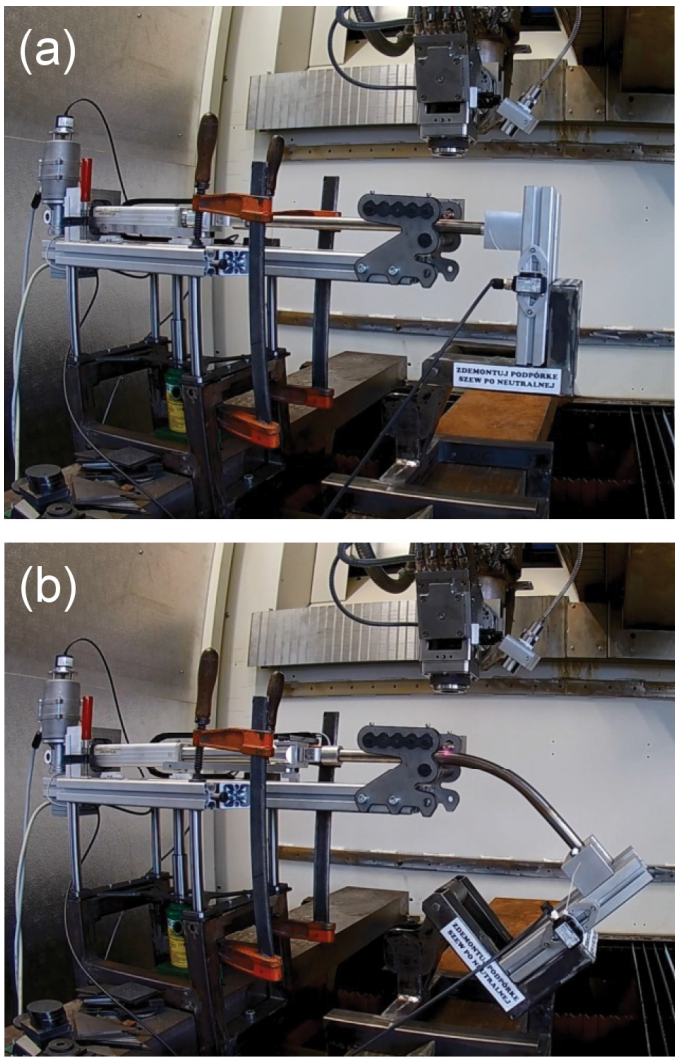

Fig. 3. Laser-assisted tube bending process: (a) the initial stage and (b) the final stage (photos taken with the 'fish-eye' lens)

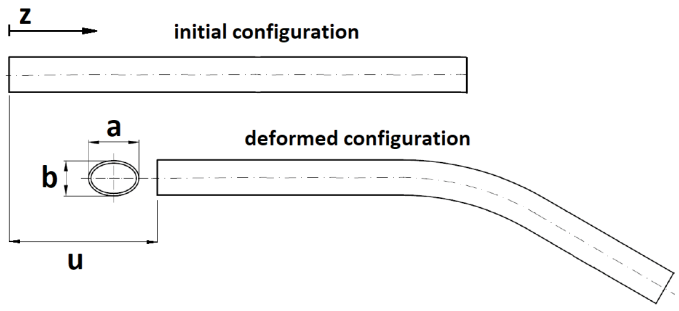

Fig. 4. Description of the initial and deformed configuration of the sample

3. Numerical simulations

The deformation of the tube during laser-assisted thermo-mechanical bending was obtained in two sequentially coupled analyses. The first one was the heat transfer analysis for a moving laser beam. In the second step the quasi-static analysis was performed taking the calculated temperature as a thermal load. All numerical simulations were performed using the ABAQUS 2016 FE program. The part of heat generated by plastic deformation of the tube's material has been neglected, as much smaller than the heat input from the laser beam. Symmetry of the object, its boundary conditions, thermal and mechanical loading as well as material isotropy was utilized in numerical modelling. Only one half of the geometry was modelled.

Rollers (labeled "7" in Fig. 1) were treated as rigid bodies because of their much higher stiffness in comparison to the stiffness of the thin-walled profile being bent. They were modelled using the 3D, 4-node, bilinear quadrilateral rigid elements of type R3D4.

In an introductory study, two numerical simulations of the cold bending problem were performed using: (1) shell elements of type S4R and (2) 3D elements of type C3D8R. The total number of elements in these analyses was 12199 and 38371, respectively. The obtained characteristics for the forming force of the actuator vs. displacement of the tube were practically the same.

The final finite element mesh for the entire model (Fig. 7) was generated in the Abaqus CAE program. The tube mesh consisted of 48960 linear hexahedral elements of type C3D8R (Abaqus/Standard Library). Four elements were assumed through the material thickness in order to effectively model the heat transfer and local bending effects. No systematic mesh convergence study was performed as numerical results in this research were verified with experimental measurements.

Thermal conductivity, specific heat, thermal expansion coefficient, Young's modulus, Poisson's coefficient [20-23] and stress-strain characteristic [24] of the material were taken as temperature-dependent (Figs. 6). The applied material data have been successfully verified in research on precise non-contact micro-positioning using the laser beam [25] and on laser-mechanical bending of thin bars [26]. An isotropic, elastic-plastic constitutive model with the Huber-Mises-Hencky (HMH) yield condition and isotropic hardening was adopted.

3.1. Heat transfer analysis

The moving laser beam was modelled as a surface heat flux using dedicated user subroutine DFLUX. In the heat transfer analysis, the displacement of the center of the laser spot was assumed to be the same as the displacement of the tube, but in the opposite direction. Hence, the laser beam did not change its position in the global reference system during the process.

The cosine law, which relates the surface intensity of radiation with the incident angle value, was respected in modelling of the radiative heat transfer on the cylindrical surface of the tube.

$$I(\alpha) = I_0 \cos(\alpha) \tag{1}$$

where: α – angle of incidence; I_0 and $I(\alpha)$ – surface intensity of radiation for the angle of incidence equal 0 and α, respectively.

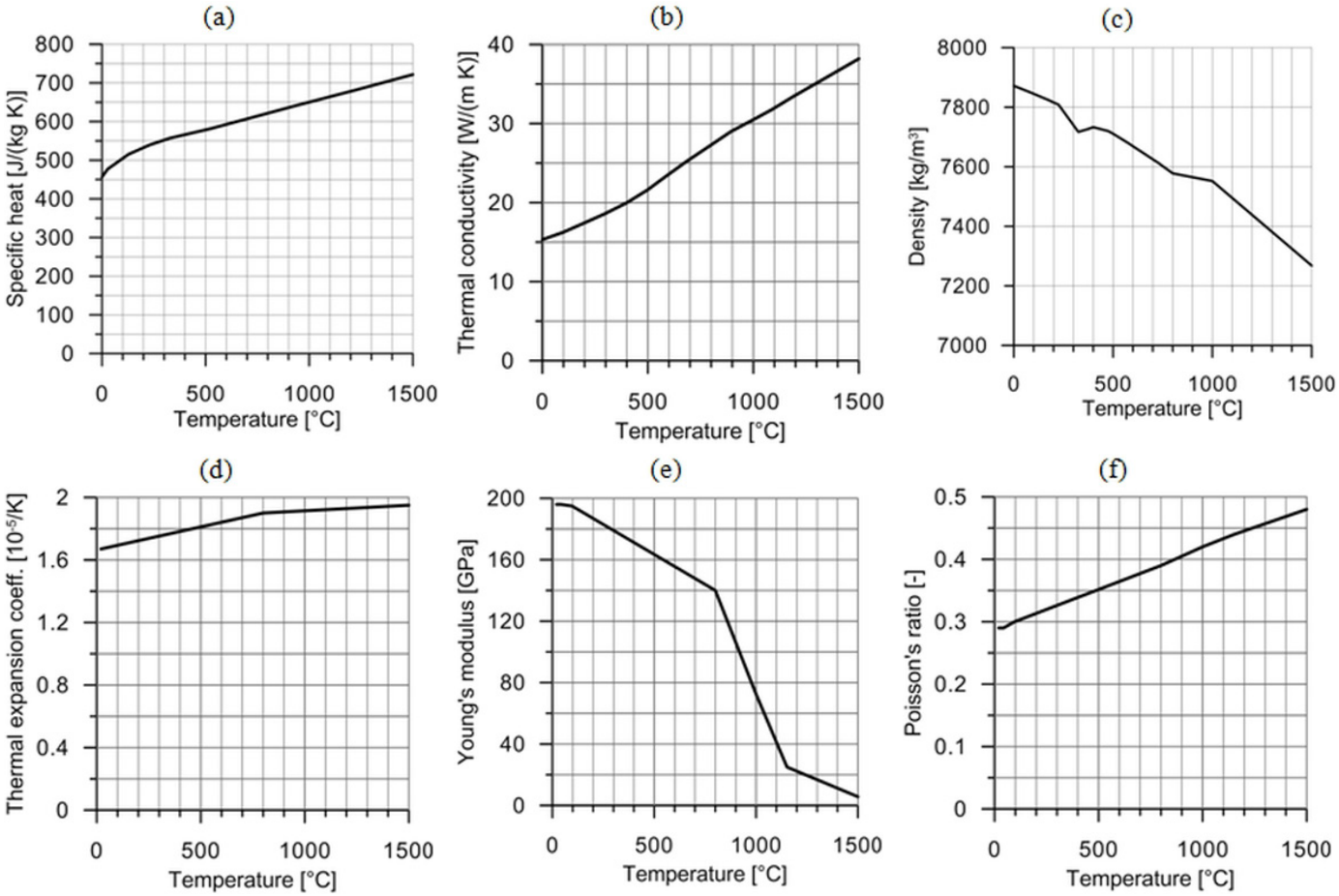

Fig. 5. Material data employed in numerical simulations [20-23]

The gaussian distribution together with cosine low were applied to model the surface power density due to laser heating.

$$I(x,\ z) = A\cos(\alpha)I_0\ \exp\left(-\frac{(z-z_C)^2}{(z_w)^2}\right) \tag{2}$$

$$\cos(\alpha) = \sqrt{1-\left(\frac{2x}{D}\right)^2} \tag{3}$$

where: A – the coefficient of radiation absorption (A = 0.36 [18,27]), z_w – parameter of the gaussian distribution (z_w = 1 mm), z_C – current z-position of the centre of the laser spot, D – diameter of the tube (D = 20 mm).

The resulting distribution of radiation surface intensity is shown in Fig. 8. The value of radiation intensity I_0 was obtained by the trial-and-error method, i.e. by performing a series of heat transfer simulations and comparing calculated temperatures with those measured with the pyrometer during experiments.

Heat dissipation due to convection and radiation was accounted for in modelling of boundary conditions in the heat transfer problem. Convective heat loss was described with Newton's law and using the heat convection coefficient value 30 W/(m^2 K). This relatively high value was assumed to take into account intensive blow of a gas stream applied to protect the optical head of the laser. The Stefan-Boltzmann law was used for the radiative heat transfer.

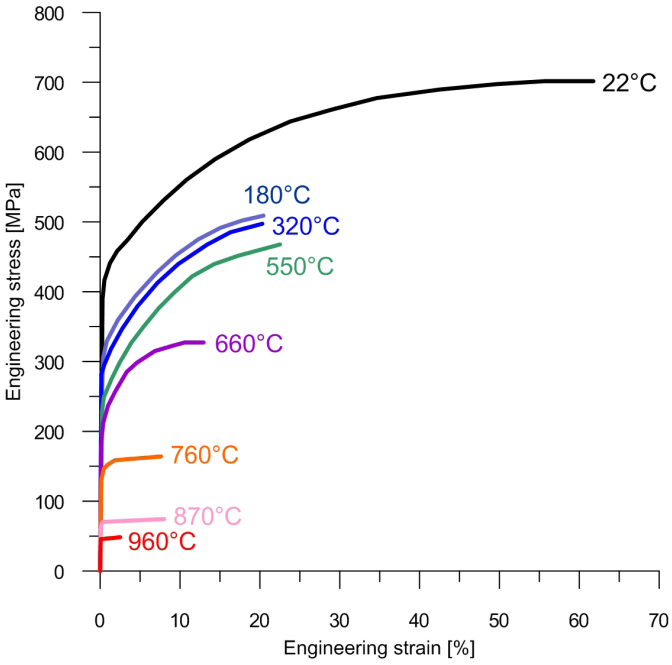

Fig. 6. Stress-strain curves [24] adopted in numerical modelling

The heat transfer analysis was defined on the initial configuration of the tube. The laser beam spot was initially placed at a distance of 50 mm from the end of the tube. Then it moved

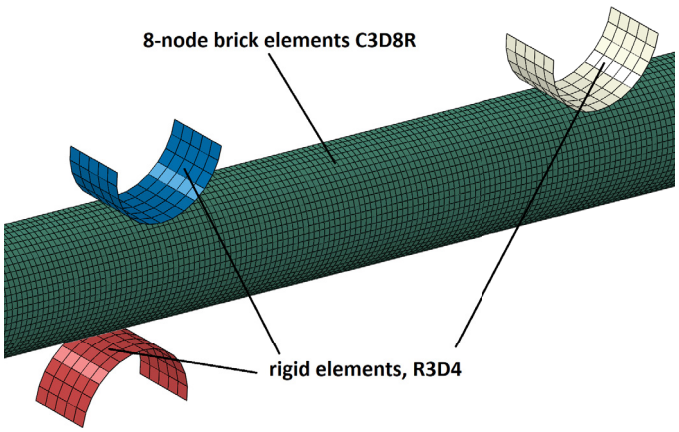

Fig. 7. A part of the finite element mesh

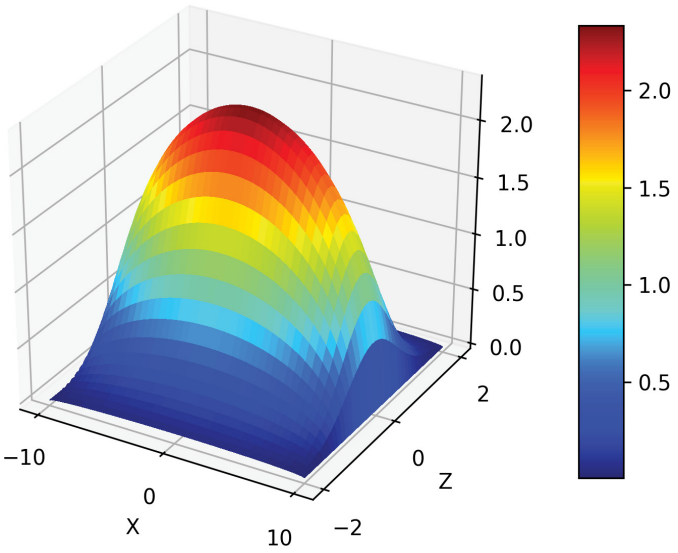

Fig. 8. Distribution of radiation surface intensity [W/(mm)^2] in the local reference frame of the laser spot

towards the other end of the tube. The results of heat transfer analysis for selected time instances are shown in Fig. 9. The consecutive stages of heating show a similar temperature dis-

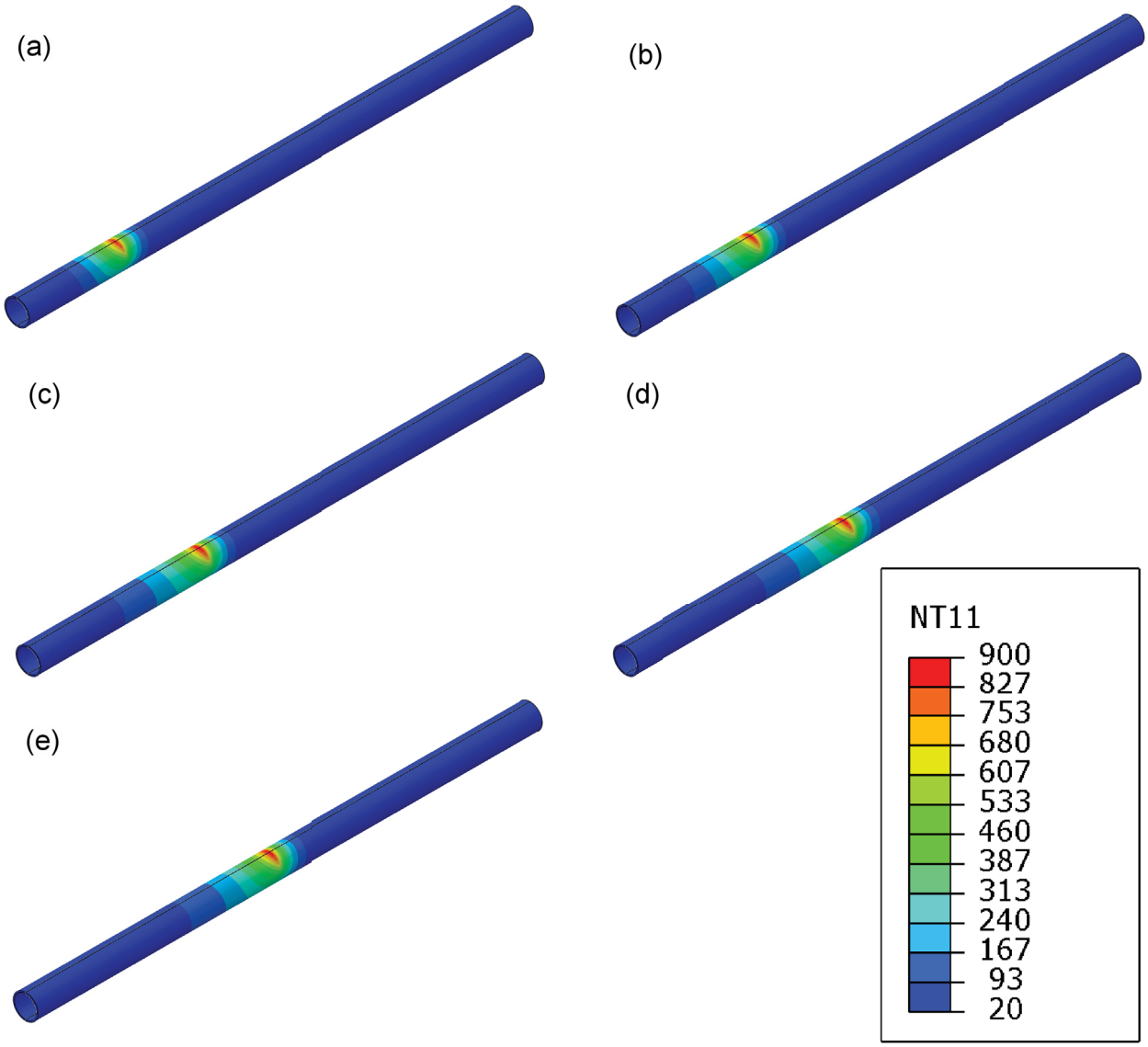

Fig. 9. The temperature distribution during laser heating on the outer surface of tube for time instants: (a) t = 20 s, (b) t = 40 s, (c) t = 80 s, (d) t = 120 s, (e) 140 s

tribution in the reference frame of the laser spot. Therefore, the temperature distribution from the beginning of the process can be shifted according to the beam motion and the process can be considered as a steady one in the reference frame of the heat source.

3.2. Quasi static analysis of tube bending

Figure 10 shows the kinematic model of the experimental stand and the applied boundary conditions. The actuator (9) was modelled as a connector element with a prescribed displacement history. One end of the actuator was fixed (10) and the other one (8) was rigidly connected to the tube with the use of the multi-point constraint MPC. The tube (7) was modelled as a three-dimensional body. Its length was 400 mm, diameter 20 mm and thickness of the wall 0.9 mm. The value of the wall thickness employed in numerical calculations was chosen close to the minimal measured thickness of the actual samples in order to obtain the upper estimate of unwanted deformations, that accompany the bending process.

The tube was placed between guiding rollers (4, 5, 6) modelled as discrete rigid bodies. The end of the tube (3) was attached to the bending arm (2), which was modelled as a connector element. The bending arm could freely rotate around the point (1), as a hinge-type element.

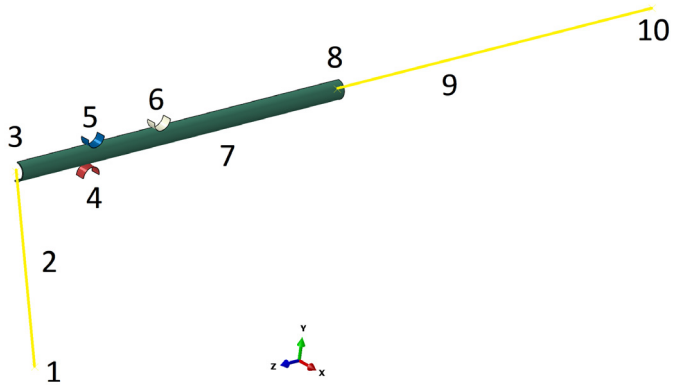

Fig. 10. The applied boundary conditions for the tube bending process 1 – rotation point (hinge element), 2 – bending arm (connector element), 3 – MPC with hinge element, 4, 5, 6 – horizontal rollers (discrete rigid body), 7 – tube, 8 – MPC with hinge element, 9 – actuator (connector element with a prescribed displacement), 10 – fixed point with hinge element

The linear penalty method was used as the contact constraint enforcement in all numerical simulations. With this method the pressure-overclosure relationship is linear, which allows for improved solver efficiency. In the applied algorithm for contact analysis, the penalty stiffness was set to 10 times representative underlying element stiffness. The tangential behavior was described using the classical isotropic Coulomb friction model. The friction coefficient value was assumed 0.1, based on additional measurements of the pushing force, which was necessary to displace the sample through the device without bending.

4. Discussion

Three types of simulations were compared with experimental results: cold bending and two cases of the laser-assisted bending with the relative velocity of the laser spot 20 and 40 mm/min, both with the temperature at the laser spot set to 800°C using the automatic laser power control system. The experimental and calculated force-displacement curves are shown in Fig. 11.

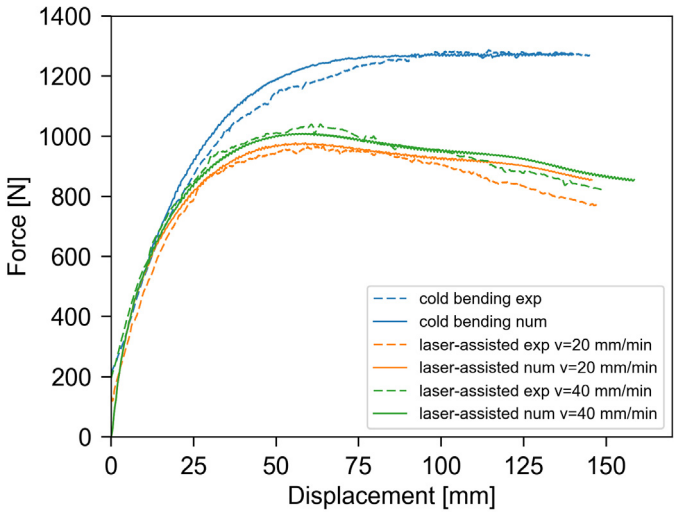

Fig. 11. A comparison of experimental and numerical results

While the applied numerical model described the ideal initial geometry of the sample and its loading system, the real conditions were slightly different, including: (1) variability in the wall tube thickness, (2) some backlash existing in the involved kinematic pairs, (3) the finite stiffness of the experimental setup. The latter factor can contribute, in particular, to the discrepancy of experimental and numerical force-displacement curves during the final phase of the bending process. As the pyrometer was fixed to the laser head (Fig. 2), a small vertical displacement of the sample with respect to the laser head resulted in a considerable displacement of the temperature measurement location from the centre of the laser spot, towards the cooler neighbourhood. A similar problem occured in the research on laser tube forming with axial pre-loads [16]. Under the applied close-loop temperature control system, such misalignment of the laser spot and the temperature measurement field leads to the automatic increase of laser power and, consequently, to an increase of temperature at the centre of laser spot above the desired value. Finally, thermal softening of the material is increased. This effect can explain why the required forming force in the final phase of the laser-assisted bending process was smaller in experimental measurements than in numerical calculations. Taking into account complexity of the considered thermal-elastic-plastic problem with a moving laser beam, satisfactory consistency of experimental and theoretical force-displacement results was achieved.

It is evident that a much smaller force is needed in the bending process with laser heating. The influence of the heat input also causes that the forming force is constantly decreasing

in the final phase of the process. These effects are beneficial for bending of tubes made of difficult-to-form materials.

During tube deformation process, two guiding rollers are in strong contact with the tube: (1) the bottom roller and (2) the back roller. This results in high reaction forces. The tube undergoes a strong deformation in the region of contact with the bottom roller, which causes ovalization of the tube (Fig. 12). The upper right (front) roller practically is not in contact with the tube from the beginning of the process. The distribution of Mises (HMH) equivalent stress in the workpiece indicates not only a high local mechanical loading by the bottom roller, but also a significant stressing of the tube between front rollers and the bending arm. Taking into account relatively low heat conduction coefficient value of X5CrNi18-10 stainless steel (23 W/(m K) at 600°C) as compared to the mild steel (37 W/(m K) at 600°C) and many other structural materials, the relatively large extent of highly stressed area at elevated temperature may have detrimental effect on the control of plastic forming process. To reduce the hot deformation zone, the application of forced cooling of the workpiece in the vicinity of laser spot should be considered in the further research and development process. Water cooling is successfully used in the pipe bending technique with local induction heating [28].

The normal stress σ_z distribution at the cross-section located in the plane of the front roller's axes during the laser-assisted bending process is shown in Fig. 13a. An effect of flattening and the circumferential local bending [29] can be observed as overlaid on a typical normal stress distribution in bending.

The horizontal and vertical dimensions, a and b, respectively, of the tube cross-section (Fig. 4) were extracted from numerical calculations. Ovalization of the tube can be expressed by the following formula [14]

$$e = \frac{2(a-b)}{a+b} \tag{4}$$

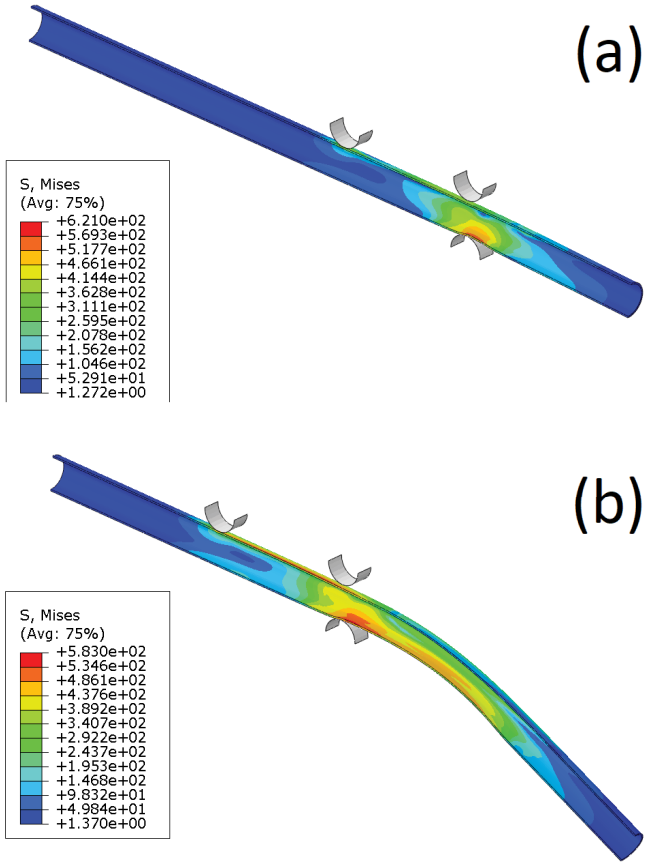

Fig. 12. The distribution of Mises (HMH) equivalent stress for the laser-assisted tube bending: (a) $t = 20.0$ s, (b) $t = 120.0$ s

Cross-sections of the tube after the cold and laser-assisted bending process are compared in Fig. 14. Coordinates $z = 0$, 100, 200, 300 and 400 mm of the cross-sections denote positions in the initial (straight) configuration of the tube (Fig. 4).

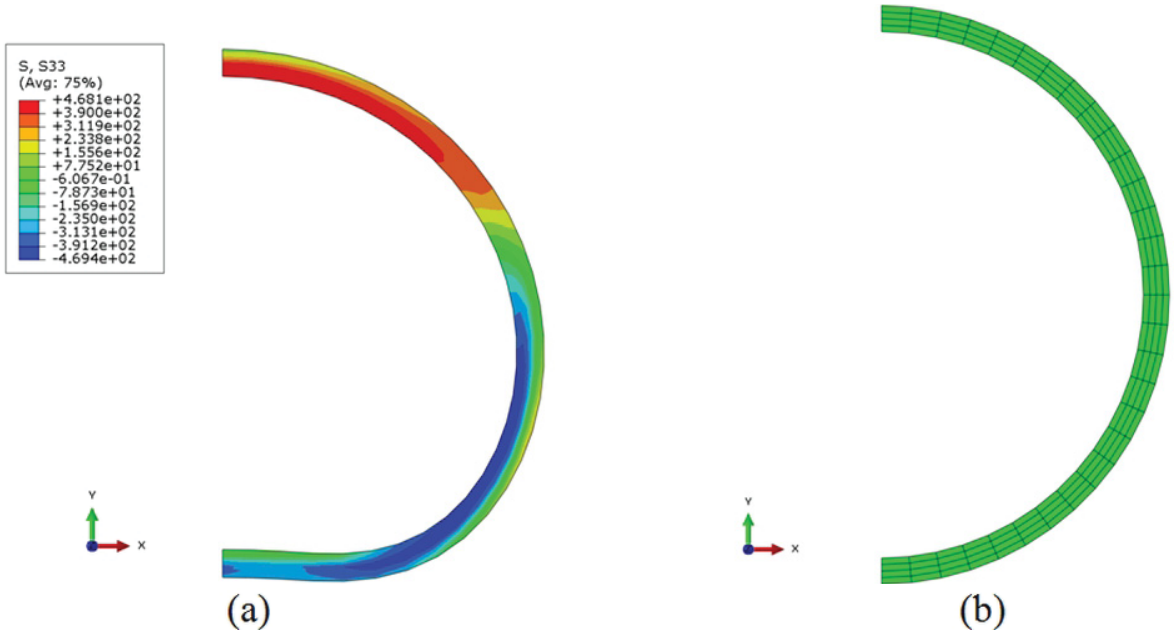

Fig. 13. Deformation and normal stress σ_z distribution at the cross-section located in the plane of front roller's axes: (a) the laser assisted bending, $t = 120$ s, (b) the initial ($t = 0$) shape with the mesh of finite elements

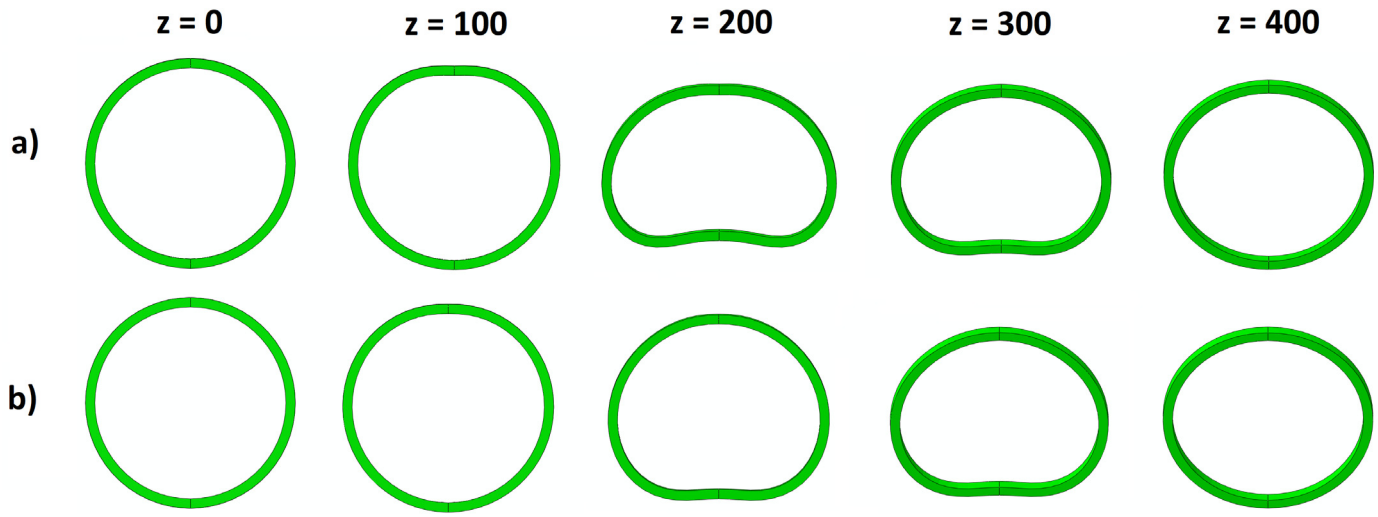

Fig. 14. Cross-sections of the tube at selected locations z after the bending process: (a) cold bending, (b) laser-mechanical bending

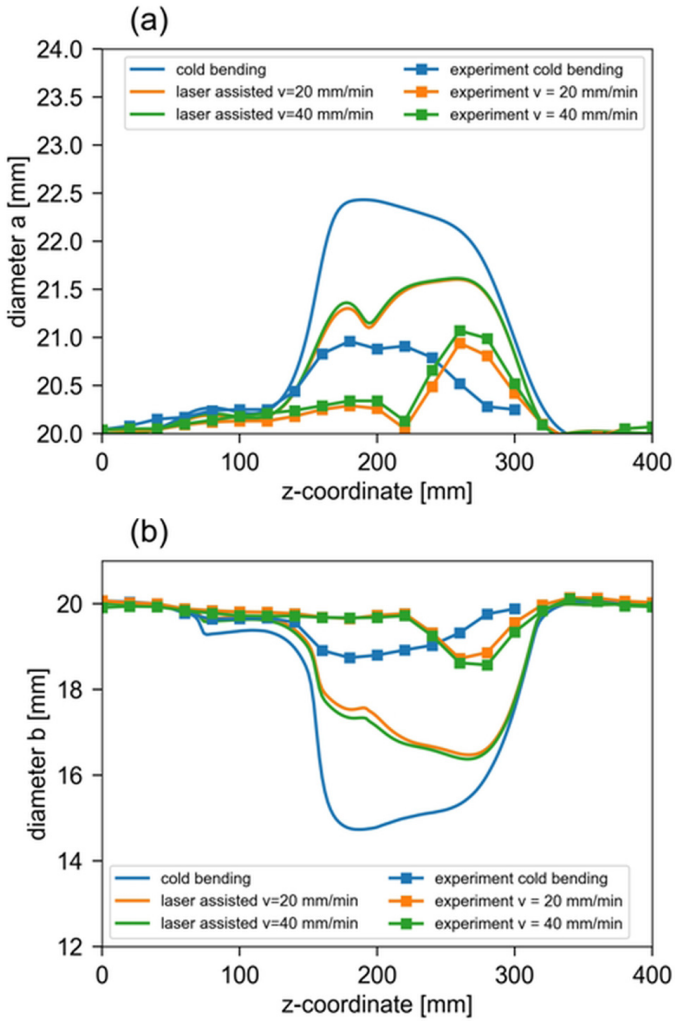

Fig. 15. A comparison of cross-sectional dimensions of the tube along its length after the deformation process: (a) the horizontal dimension, (b) the vertical dimension

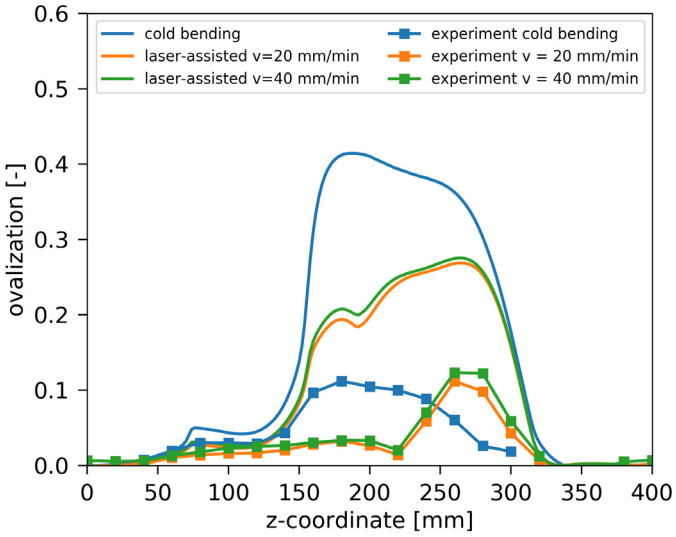

Fig. 16. A comparison of the ovalization for the three studied cases

The flattening of the profile in numerical calculations is generally larger than in experimental investigation. There is a considerable discrepancy between the numerical and experimental results for cross-sectional deformation (Fig. 15) and ovalization (Fig. 16). A similar relation regarding thermo-mechanically induced deformation occurred also in [16]. One of the possible reasons for that may be the conservative assumption regarding the wall thickness, which was assumed in the numerical model. However, the trends in calculated and measured results are similar, which suggests that a slight increase in the wall thickness in numerical simulations can reduce the discrepancy, as the stiffness of the profile cross-section significantly depends on the wall thickness.

An interesting effect can be seen in experimental data concerning the ovalization value within the range $z = 150$ to 240 mm (Fig. 16). The ovalization produced in laser-mechanical bending is considerably smaller (up to about three times) than the one measured after the cold bending process. Further research and optimization of the thermo-mechanical process can result in improving the ovalization over the whole curved portion of the bend.

The final deformation after spring-back is depicted in Fig. 17. The upper part of the figure shows the real image of

the final deformation of the tube. For a comparison, the configuration obtained from numerical simulation is placed below. For all three analysed cases, significant ovalization occurred in cross-sections that were in contact with the rollers during the deformation process (Fig. 16). A slight local flattening can be seen even due to the contact with the upper back roller (Fig. 14a, $z = 100$). The maximum value of measured ovalization is similar for the cold and laser-assisted bending. The unwanted deformation was smaller after heating with the smaller relative laser spot velocity (20 mm/s).

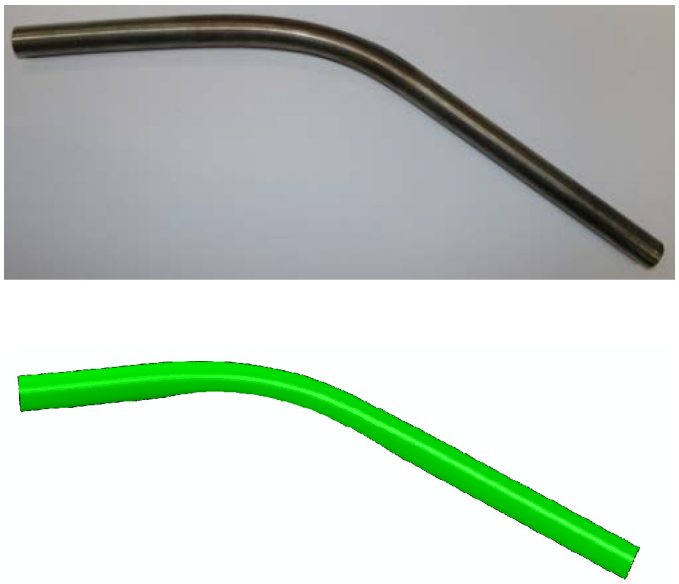

Fig. 17. An example of final deformation of the tube after laser-assisted bending process, top – experiment, bottom – numerical simulation

5. Summary and conclusions

The proposed method of laser assisted thermo-mechanical bending has been analysed, both experimentally and numerically. The work proved that laser heating can be successfully used in the forming process for thin-walled profiles. The applied method and experimental setup allow flexible bending of tubes [8] within a range of diameters, wall thickness, bending radii and bend angles, without requiring different tool sets.

The heat transfer analysis with a moving laser beam showed that the process of heating can be treated as a steady one in the reference system associated with the heat source. Ovalization of the tube cross-section was observed as a consequence of a relatively large contact force between tube and the bottom roller. Numerical results show a good agreement with the experimental values regarding the force-displacement curve. The use of a laser beam reduces the pushing force by about 35% in comparison with the cold bending process. This effect may be of great importance for bending tubes made of difficult-to-form materials. Application of the two times lower relative laser spot velocity (20 mm/s vs. 40 mm/s) with the same material temperature value 800°C set for the laser power control system resulted in a further decrease of the required forming force, although the change was small. With a lower velocity of the heat source, under the same peak temperature, the extent of thermo-plastic deformation zone is larger.

The differences between measured and calculated cross-sectional dimensions and ovalization values seem to result from using a smaller wall thickness value in numerical modelling than the average from measurements taken on real samples.

To ensure reliable temperature measurements for the closed-loop laser power control system, a better alignment of the pyrometer with the laser spot or the application of the field measurement with an IR camera should be considered for the future investigations. Thermal imaging can significantly improve the process monitoring and control.

Acknowledgement

The research reported herein was supported by a grant from the National Centre for Research and Development (No. PBS3/A5/47/2015).

REFERENCES

[1] J. Michalczyk, K. Wojsyk, Development and Modelling of the Method of Mandrel-less Small-Radius Tube Bending, Arch. Metall. Mater. **60** (4), 2797-2803 (2015).

[2] N.C. Tang, Plastic-deformation analysis in tube bending, International Journal of Pressure Vessels and Piping **77**, 751-759 (2000).

[3] H. Yang, Y. Lin, Wrinkling analysis for forming limit of tube bending processes, Journal of Materials Processing Technology **152**, 363-369 (2004).

[4] H. Frackiewicz, Forming metal pipe and tube with laser. High--power optical beam method developed for fabricators, The Tube and Pipe Quarterly **3**, 3 (1992).

[5] H. Frackiewicz, W. Trampczynski, W. Przetakiewicz, Shaping of Tubes by Laser Beam, Proc. of the 25th ISATA 373-380 (1992).

[6] Z. Mucha, J. Widłaszewski, M. Cabaj, R. Gradoń, Surface temperature control in laser forming. Archives of Thermodynamics **24** (2), 89-105 (2003).

[7] Z. Mucha, J. Widłaszewski, Physical Foundations of Laser Thermal Forming, Proceedings of the 1st International Conference on New Forming Technology, ICNFT. Eds.: Wang Z.R., Dean T.A., Yuan S.J., Harbin Institute of Technology Press 235-240, 2004.

[8] J.M. Allwood, H. Utsunomiy, A survey of flexible forming processes in Japan. International Journal of Machine Tools & Manufacture **46**, 1939-1960 (2006).

[9] W. Zhang, J. Marte, D. Mika, M. Graham, B. Farrell, M. Jones, Laser forming: Industrial applications, ICALEO 2004 – 23rd International Congress on Applications of Laser and Electro- Optics, Congress Proceedings (2004).

[10] W. Zhang, M. Jones, M. Graham, B. Farrell, M. Azer, C Erikson, J. Zhang, Y.L. Yao, Large diameter and thin wall laser tube bending, ICALEO 2005 - 24th International Congress on Applications of Lasers and Electro-Optics, Congress Proceedings 64-73 (2005).

[11] H. Li, H. Yang, Z.Y. Zhang, G.J. Li, Multiple instability-constrained tube bending limits, Journal of Materials Processing Technology **214**, 445-455 (2014).

[12] E. Simonetto, G. Venturato, A. Ghiotti, S. Bruschi, Modelling of hot rotary draw bending for thin-walled titanium alloy tubes, International Journal of Mechanical Sciences **148**, 698-706 (2018).

[13] Z. Hu, J.Q. Li, Computer simulation of pipe-bending processes with small bending radius using local induction heating, Journal of Materials Processing Technology **91**, 75-79 (1999).

[14] M. Cieśla, R. Findziński, G. Junak, T. Kawała, The effect of heat treatment parameters on mechanical characteristics of 10CrMo9-10 steel tube bends, Archives of Metallurgy and Materials **60** (4), 2971-2976 (2015).

[15] A. Kratky, Laser Assisted Forming Techniques. XVI International Symposium on Gas Flow, Chemical Lasers, and High-Power Lasers, edited by Dieter Schuöcker. Proceedings of SPIE **6346**, 634615, (2007).

[16] Hsieh H.-S., Lin J., Study of the buckling mechanism in laser tube forming with axial preloads. International Journal of Machine Tools and Manufacture **45**, 1368-1374 (2005).

[17] M.C. Jamil., E.I. Fauzi, C.S. Juinn, M.A. Sheikh, Laser bending of pre-stressed thin-walled nickel micro-tubes. Opt. Laser Technol. **73**, 105-117 (2015).

[18] J. Widłaszewski, M. Nowak, Z. Nowak, P. Kurp, Laser-assisted forming of thin-walled profiles Metal Forming **28**, 3, 183-198 (2017).

[19] P. Kurp, J. Widłaszewski, Z. Mucha, Laser-mechanical hybrid forming of thin-walled elements. 27th International Conference on Metallurgy and Materials – METAL 2018, Brno, Czech Republic, 23-25 May, 2018. Conference Proceedings, 407-412. ISBN 978-80-87294-84-0.

[20] H.-S. Hsieh, J. Lin, Laser-induced vibration during pulsed laser forming. Optics & Laser Technology **36**, 431-439 (2004).

[21] V.V. Frolov, V.A. Vinokurov, W.N. Volczenko, V.A. Parachin, I.A. Arutionova, Theoretical fundamentals of welding (Teoreticheskie osnovy svarki – in Russian). Izdatel'stvo Vysshaya Shkola, Moscow (1970).

[22] L. Colombier, J. Hochmann, Stainless and Heat-Resisting Steels. Edward Arnold, London, UK (1967).

[23] C.S. Kim, Thermophysical properties of stainless steels. Technical Report ANL-75-55. Argonne National Laboratory, Argonne Ill., 1-24 (1975).

[24] J. Chen, B. Young, Stress-strain curves for stainless steel at elevated temperatures. Engineering Structures **28**, 229-239 (2006).

[25] J. Widłaszewski, The effects of design parameters on the laser--induced in-plane deformation of two-bridge actuators. International Journal of Machine Tools and Manufacture **80-81C**, 30-38 (2014).

[26] Z. Mucha, J. Widłaszewski, P. Kurp, K. Mulczyk, Mechanically-assisted laser forming of thin beams, Proc. of SPIE, **10159** (2016).

[27] Z. Nowak, M. Nowak, J. Widłaszewski, P. Kurp, Experimental and numerical investigation on laser-assisted bending of pre-loaded metal plate. AIP Conference Proceedings, American Institute of Physics, 1922, 140006 (2018).

[28] X.-t. Li, M.-t. Wang, F.-s. Du, Z.-q. Xu, FEM Simulation of Large Diameter Pipe Bending Using Local Heating. Journal of Iron and Steel Research International **13**, 5, 25-29 (2006).

[29] T. Welo, F Paulsen, Predicting Tube Ovalization in Cold Bending: An Analytical Approach. Key Engineering Materials **651-653**, 1146-1152 (2015).